Dual Mode of Action for Plusbacin A$_3$ in *Staphylococcus aureus*

Robert D. O'Connor[†], **Manmilan Singh**[†], **James Chang**[‡], **Sung Joon Kim**[‡], **Michael VanNieuwenhze**[§], and **Jacob Schaefer**[*,†]

[†]Department of Chemistry, Washington University, St. Louis, Missouri 63130, United States

[‡]Department of Chemistry and Biochemistry, Baylor University, Waco, Texas 76798, United States

[§]Department of Chemistry, Indiana University, Bloomington, Indiana 47405, United States

Abstract

We have used C{F}, N{F}, and N{P} rotational-echo double resonance NMR to determine the location and conformation of ^{19}F and ^{15}N double-labeled plusbacin A$_3$ and of double-labeled *deslipo*-plusbacin A$_3$, each bound to the cell walls of whole cells of *Staphyloccocus aureus* grown in media containing [1-^{13}C]glycine. The ^{31}P is primarily in wall teichoic acid. Approximately 25% of plusbacin headgroups (the cyclic depsipeptide backbone) are in a closed conformation (N–F separation of 6 Å), while 75% are in a more open conformation (N–F separation of 12 Å). The closed headgroups have no contact with wall teichoic acid, whereas the open headgroups have a strong contact. This places the closed headgroups in hydrophobic regions of the cell wall and the open headgroups in hydrophilic regions. None of the plusbacin tails have contact with the ^{31}P of either wall teichoic acid or the cell membrane and thus are in hydrophobic regions of the cell wall. In addition, both heads and tails of plusbacin A$_3$ have contact with the glycyl ^{13}C incorporated in cell-wall peptidoglycan pentaglycyl bridges *and* with ^{13}C-labeled purines near the membrane surface. We interpret these results in terms of a dual mode of action for plusbacin A$_3$: *first*, disruption of the peptidoglycan layer nearest to the membrane surface by closed-conformation plusbacin A$_3$ leading to an inhibition of chain extension by transglycosylation; *second*, thinning and disruption of the membrane (possibly including disruption of ATP-binding cassette transporters embedded in the membrane) by open-conformation plusbacin A$_3$, thereby leading to release of ATP to the hydrophilic regions of the cell wall and subsequent binding by plusbacin A$_3$.

Graphical abstract

[15N, 19F]plusbacin A3
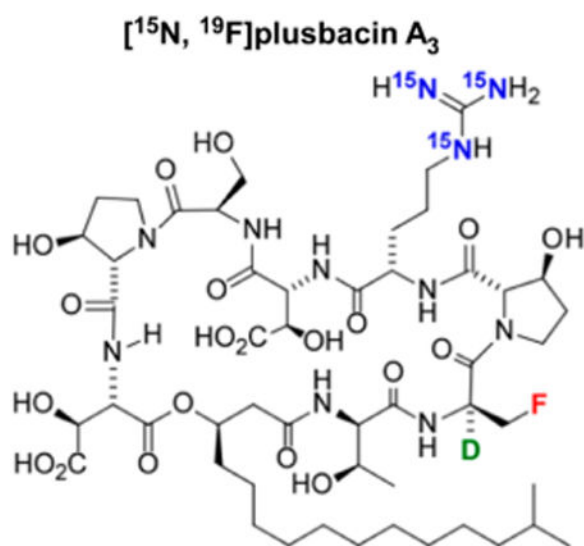
Introduction

Plusbacin A_3 is a cyclic lipodepsipeptide produced[1] by *Pseudomonas* sp. PB-6250.
Plusbacin A_3 exhibits potent antimicrobial activities[2] against Gram positive bacteria
including methicillin-resistant *Staphyloccocus aureus* (MRSA) and vancomycin-resistant
enterococci (VRE). Plusbacin A_3 has a structural motif commonly found in cyclic
antimicrobial peptides: a cyclic-peptide core and a lipophilic side chain.[3] The cyclic core in
plusbacin A_3 has eight amino acids cyclized through a lactone linkage between L-threo-β-
hydroxyaspartic acid and a hydroxyl fatty acid subunit. The core is modified by attachment
of an isotridecanyl side chain. A similar motif, *deslipo*-plusbacin A_3, has no side chain
(Figure 1) and no antimicrobial activity.[4]

Plusbacin A_3 inhibits cell-wall synthesis in Gram positive bacteria by blocking the
incorporation of N-acetylglucosamine in nascent peptidoglycan.[5] The addition of cell-
membrane precursors antagonizes this activity which suggests that plusbacin A_3 targets
peptidoglycan biosynthesis. The mode of action was further characterized by solid-state
NMR experiments on intact whole cells of *S. aureus* grown in the presence of subinhibitory
concentrations of the drug added during midexponential growth.[4] The resulting *S. aureus*
showed an accumulation of Park's Nucleotide, the inhibition of D-alanine incorporation into
cell-wall teichoic acids, and no effect on peptidoglycan cross-linking. These effects are
identical to those of a well-known transglycosylase inhibitor, vancomycin, confirming that
plusbacin A_3 targets the transglycosylation step of peptidoglycan biosynthesis.[6] However,
unlike vancomycin, plusbacin A_3 activity is not inhibited by the addition of tripeptide acetyl-
L-Lys-D-Ala-D-Ala.[2] In addition, plusbacin A_3 is active against VRE. This indicates that
plusbacin A_3 does not target lipid II but has a different binding site. C{D} rotational-echo
double resonance (REDOR) NMR of whole cells of *S. aureus* grown in media containing
[1-^{13}C]glycine confirmed that the isotridecanonyl side chain of a plusbacin A_3 with a ^{2}H-
labeled isopropyl subunit is near the pentaglycyl bridge of cell-wall peptidoglycan.[4] There
was no evidence of contact of the side chain with membrane aliphatic carbons or lipid head-

groups, the latter conclusion based on P{D} REDOR. That is, the plusbacin A_3 side-chain tail did not penetrate the membrane bilayer.[4]

In this report, we detail the results of various REDOR experiments designed to locate plusbacin A_3 within the cell and to determine its local structure. Both [^{15}N, ^{19}F]plusbacin A_3 and [^{15}N, ^{19}F]*deslipo*-plusbacin A_3 (Figure 1) were examined, each bound to the cell walls of whole cells of *S. aureus* grown in media containing [1-^{13}C]glycine. The ^{15}N and ^{19}F labels were inserted in the cyclic-core headgroup using ^{15}N-guanadino labeled L-arginine and D-[^{2}H, ^{19}F]alanine. The deuterium label was not used in these experiments.

Materials and Methods

Synthesis of Plusbacin A₃ Analogues

The detailed chemical syntheses of plusbacin A_3 and *deslipo*-plusbacin A_3 have been presented earlier.[4] The labeled drugs of Figure 1 were synthesized using L-[^{15}N$_3$]arginine (Isotec, Miamisburg, OH) and L-[2-^{2}H, 3-^{19}F]alanine (Merck, Rahway, NJ).

Growth and Labeling of Whole Cells and Formation of the Drug Complex

Overnight cultures of *S. aureus* (ATCC 6538P) grown in 5 mL of trypticase soy broth at 37 °C with 250 rpm shaking were used to inoculate a 1 L flask, containing 250 mL of defined media.[7] The defined media contained isotope-labeled [1-^{13}C]glycine to incorporate ^{13}C-specific labels at the pentaglycyl cross bridge of the peptidoglycan. The cells were harvested at OD_{660nm} 1.0–1.2 (yields of approximately 100 mg dry weight) and then resuspended in 15 mL of deionized water to which was added 7 mg of double-labeled plusbacin A_3 or *deslipo*-plusbacin A_3 with gentle stirring. (DMSO was included in the plusbacin A_3 preparation to aid water solubility.) The concentration of drug per cell corresponded to approximately 2 μg/mL of drug added to cells grown to OD_{660nm} 0.1 in a 1 L flask. The whole cells of *S. aureus* complexed with drug were allowed to equilibrate for 5 min on ice. The mixture was then frozen using liquid N_2 and lyophilized.

Solid-State NMR

The C{F}, N{F}, and N{P} REDOR spectra[8] were acquired using an 89 mm bore, 12 T static field (^{1}H at 500 MHz, Magnex, Agilent, Santa Clara, CA, USA) with a Tecmag (Houston, TX, USA) Apollo spectrometer, and four channel transmission-line probes equipped with 5 mm Chemagnetics/Varian stators and zirconium thin-wall rotors containing approximately 150 mg of complexed whole cells. Radio frequency pulses for ^{1}H and ^{19}F were amplified first by 50 W American Microwave Technology (AMT, Anaheim, CA, USA) power amplifiers and then by 2 kW Creative Electronics tube amplifiers. AMT amplifiers (1 kW) were used for ^{15}N and ^{13}C pulses. The π-pulse lengths were 7 μs for ^{13}C, ^{15}N, and ^{19}F and 6 μs for ^{31}P. The ^{1}H decoupling field was 100 kHz throughout dipolar evolution and data acquisition with TPPM of the ^{1}H radio frequency.[9] The spinning rates (either 7143 or 8000 Hz) were actively controlled to ±2 Hz. All radiofrequency field amplitudes were under active control to eliminate long-term drifts due to component aging or changes in temperature.[10] Additionally, alternating scans of S_0 and S were acquired to compensate for short-term drift. XY-8 phase cycling[11] was used for all refocusing and dephasing pulses.[12]

The ^{13}C chemical shifts were referenced to external TMS, and the ^{15}N chemical shifts, to external solid ammonium sulfate. Carbon spectra typically involved 64,000 scans (3 days), and nitrogen spectra, 200,000 scans (10 days).

Internuclear Proximities

REDOR was used to determine dipolar couplings and hence internuclear distances.[13] REDOR is a difference experiment in which two spectra are collected, S_0 (full echo) and S (dephased echo). Dipolar evolution over one or more rotor periods in the S spectrum results in reduced (dephased) peak intensity for spin pairs that are dipolar coupled. From the difference in signal intensity (REDOR difference, $\Delta S = S_0 - S$) and the experimental dephasing time (the dipolar evolution time), the heteronuclear dipolar coupling and corresponding internuclear distance can be directly calculated.[8] REDOR calculations were based on the analytical expressions of Mueller et al.[13]

Statistical Testing of Multiparameter Fitting of REDOR Dephasing

Often single distances do not yield good fits to the experimental REDOR dephasing and more complicated models based on weighted distributions of internuclear distances must be adopted. This is the situation for the plusbacin-whole-cell complexes reported here. The Levenberg–Marquardt nonlinear least-squares method[14] was used to fit the models to the data with a goodness-of-fit measure

$$\chi^2 = \sum_i^n (1 - \langle \Delta S/S_0 \rangle_{i,\text{calc}} / \langle \Delta S/S_0 \rangle_{i,\text{exp}})^2$$

where $\langle \Delta S/S_0 \rangle_i$ is the ith of n REDOR calculated or experimental dephasing values.

Model-hypothesis testing was based on an F-test at the 99% significance level.[15] This test uses an F-statistic to compare the relative decrease in minimized χ^2 to the relative increase in the degrees of freedom (the number of variable parameters) between a (complicated) trial model and a (simple, single-distance) reference model. The F-statistic is $(n - np_{\text{trl}})(\chi_{\text{ref}}^2 - \chi_{\text{trl}}^2)/(np_{\text{trl}} - np_{\text{ref}})\chi_{\text{trl}}^2$, where n, np_{trl}, and np_{ref} represent the number of data points, the number of trial-model variable parameters, and the number of reference-model variable parameters, respectively. If the F-statistic is greater than the published critical value of the F-distribution,[16] $F_{0.01}(np_{\text{trl}} - np_{\text{ref}}, n - np_{\text{trl}})$, then with 99% confidence, the trial model represents the data better than the reference model.

Double REDOR

The pulse sequence for N{P}{F} double REDOR is shown in Figure 2. The ^{19}F dephasing pulses (dotted, on for S and off for S_0) follow the ^{31}P dephasing pulses (on for both S and S_0). The wait time can be used as an optional $T_1(N)$ filter. The purpose of this experiment is to test whether ^{15}N labels that are proximate to ^{19}F are also proximate to ^{31}P. If so, then the N{P}{F} $\Delta S/S_0$ will be less than the N{F} $\Delta S/S_0$ for the same dipolar evolution time.

Results

N{F} REDOR

The ^{15}N NMR full-echo spectrum of double-labeled plusbacin bound to whole cells of *S. aureus* has a peptide-nitrogen peak near 95 ppm and an arginyl side chain nitrogen doublet centered at 50 ppm (Figure 3, bottom). The former arises from natural-abundance ^{15}N (0.37% isotopic concentration) and the latter from NH_2 and NH arginyl ^{15}N labels (99% isotopic enrichment). After a T_2 correction, the arginyl peak has 3 times the integrated intensity of the peptide peak.

Whole cells of *S. aureus* are about 50% protein and peptide (dry weight, including the cell wall). For a 100 mg sample, this translates to about 500 μmol of residues (average molecular weight of 100 mg/mmol with 1.2 nitrogens per residue). The protein and peptide have approximately 250 units of ^{15}N signal intensity ($500 \times 0.37 \times 1.2 \approx 250$). A 7 mg (6 μmol) sample of double-labeled plusbascin was complexed to the whole cells, which should generate approximately 1800 units of ^{15}N signal intensity ($6 \times 99 \times 3 \approx 1800$). That is, the label intensity (near 50 ppm) should be 7 times that of the natural-abundance peptide peak (near 90 ppm) but it is only 3 times. We attribute the diminution of the label peak intensity to losses in handling small quantities of the hydrophobic plusbacin while making the complex.

Only the arginyl peak contributes to a N{F} REDOR difference spectrum (Figure 3, top). As a function of evolution time, the N{F} REDOR difference for double-labeled plusbacin A_3 is slightly greater but comparable to that for the corresponding *deslipo*-plusbacin A_3 complex (Figure 4). Neither dependence can be described in terms of a single N–F distance (Figure 4, dotted lines). A suitable fit is obtained for two distances, one about 5–6 Å and the other 12 Å. The quality of the fit is improved if each is distributed, the shorter distance with a broader (variable) distribution reflecting heterogeneity in binding and the longer distance with a narrow (fixed) distribution reflecting more homogeneity (Figure 4, solid lines). The statistical significance of the fitting procedure will be described in detail after the C{F} results have been introduced.

C{F} REDOR

The ^{13}C NMR full-echo spectrum of double-labeled plusbacin (left) and *deslipo*-plusbacin A_3 (right) complexed to whole cells of *S. aureus* grown in media labeled by [1-^{13}C] glycine is dominated by a peptide carbonyl-carbon peak near 172 ppm (Figure 5, bottom). About half of the signal arises from glycyl residues in cytoplasmic proteins and the other half from the pentaglycyl bridge in cell-wall peptidoglycan. An additional peak at 153 ppm is due to intact glycyl insertions into purines primarily for nucleotide biosynthesis.[4] The purine peak in double-label plusbacin A_3 has a significant REDOR difference, whereas that for double-labeled *deslipo*-plusbacin is missing a significant REDOR difference (Figure 5, top).

As a function of evolution time, the 175 ppm carbonyl-carbon C{F} REDOR difference for double-labeled plusbascin A_3 is slightly less but comparable to that for the corresponding *deslipo*-plusbascin A_3 complex (Figure 6). Neither dependence can be described in terms of a single C–F distance (Figure 6, dotted lines). A suitable fit is obtained for two distances,

one about 4 Å and the other 7 Å. The quality of the fit is improved if each is distributed, both with a relatively narrow (fixed) distribution (Figure 6, solid lines).

Calculated REDOR Fitting Parameters

In addition to two distributed distances, the fitting was done by varying the relative proportions of each distribution to the total REDOR dephasing (S/S_0). This mix is described by the variable parameter f, which is the fraction of distribution 1 so that the fraction of distribution 2 is $1 - f$. (The subscript "1" is associated with fixed distributions for both carbon and nitrogen distances, and subscript "2", with fixed distributions for carbon distances but variable distributions for nitrogen distances.) Finally, the asymptotic dephasing limits are parameters. For N{F} REDOR, the dipolar coupling is intramolecular and we take the dephasing limit as a fixed 95%. For C{F} REDOR, however, the dipolar coupling is intermolecular and depends on the location of plusbacin A_3 within the cell wall so we take the dephasing limit as a variable parameter, s.

As tabulated in the color-coded table of Figure 7, the single-distance models have one parameter for N{F} REDOR and two for C{F} REDOR. The distributed two-distance models have three parameters for N{F} REDOR and four parameters for C{F} REDOR. Naturally, the more parameters used in a fitting procedure, the better the *appearance* of a proper fit. To determine the statistical significance of the fitting procedure, we used an *F*-test, as described in the Materials and Methods. The summary of *F*-test calculations (Figure 7, last column) showed that all fits are statistically significant at the 99% confidence level (*F*-test numbers exceed the corresponding critical *F*-distribution numbers given in the table footnote).

Double REDOR

The N{F} REDOR dephasing for short dipolar evolution times of double-labeled plusbacin bound to whole cells of *S. aureus* can only be associated with distance-distribution 2 (Figure 7). The 12 Å N–F separation of distance-distribution 1 makes no significant contribution to dephasing for evolution times less than 5 ms. The 8% S/S_0 for N{F} REDOR after 4.48 ms of dipolar evolution (Figure 4, blue) is matched by the dephasing for N{P}{F} double REDOR (Figure 8, right) obtained using the pulse sequence of Figure 2 with a 4.48 ms N–F dipolar evolution time. That is, even though about 40% of the ^{15}N magnetization has been removed by N{P} dephasing (see Figure 8, left) in N{P}{F} double REDOR, the N{F} dephasing is unaffected. We conclude that the nitrogens associated with distance-distribution 2 are not proximate to the ^{31}P of wall-teichoic acid in the hydrophilic regions of the cell wall, but rather, they are located within the hydrophobic tightly packed peptidoglycan lattice.

Discussion

On the basis of the results summarized in Figure 7, the plusbacin A_3 headgroup has two conformations, one closed (N–F of 5–6 Å, 25% population) and the other open (N–F of 12 Å, 75% population). The headgroup conformation is independent of whether a tail is attached.

The open-conformation head has a strong contact with wall teichoic acid (N{P} $S/S_0 =$ 40% after 22.4 ms dipolar evolution) and thus is in hydrophilic regions of the cell wall. The hydrophilic regions are loosely packed local networks which include the open spaces between tightly packed regions.[17] The closed-conformation head has weak contact with wall teichoic acid (N{P}{F} $S/S_0 =$ N{F} S/S_0) and thus is in hydrophobic regions of the cell wall. The hydrophobic regions are tightly packed, 75% cross-linked, parallel-stem peptidoglycan lattices.[17]

Multiple N–F distances were unexpected and define open and closed headgroup conformations. Multiple C–F distances were expected because the bridge has five glycyl units and so five ^{13}C-labeled carbonyl carbons. Proximity of ^{19}F to a bridge necessarily involves multiple distances.

The headgroup partitioning between hydrophilic and hydrophobic regions is consistent with the observed contact between the plusbacin head and the peptidoglycan pentaglycyl bridges, as revealed by C{F} REDOR (Figures 5–7). Only the closed-conformation plusbacin A_3 will fit within the tightly packed peptidoglycan lattice and thus be proximate to a pentaglycyl bridge. We therefore expect an asymptotic dephasing limit for C{F} REDOR of about $\frac{1}{2} \times \frac{1}{4} \times \frac{1}{3} = 4\%$, which is in agreement with the observed fitting parameter (s, Figure 7). The first factor is the percentage of labeled glycyl units in pentaglycyl bridges in whole cells[18] (the remainder is in cytoplasmic protein), the second factor is the concentration of bridges missing a cross-link[18] (to provide additional space for the headgroup), and the third factor is an estimate of the number of pentaglycyl carbonyl carbons within dephasing range for a random placement of the fluorine.[18]

The plusbacin A_3 tail is necessarily in hydrophobic regions of the cell wall. However, we know what fraction of plusbacin A_3 tails are in tightly packed hydrophobic regions (Figure 7). We therefore can now calculate an asymptotic dephasing limit (s) for C{D} REDOR of whole cells complexed to plusbacin A_3 with a [2]H-labeled tail of about $\frac{1}{2} \times \frac{1}{4} \times \frac{1}{5} = 2.5\%$, in reasonable agreement with experiments reported earlier (1% dephasing after 30 ms of dipolar evolution[4]). The first factor is again the fraction of S_0 associated with pentaglycyl bridges, the second is the 25% hydrophobic fraction of plusbacin A_3 close to bridges (Figure 7), and the third an estimate of the fraction of carbonyl carbons of the bridge within dephasing range of a randomly placed deuterated tail.[4,18]

The plusbacin A_3 tail is required for interference with transglycosylation. We believe that the head–tail combination has sufficient bulk to disrupt the organization of the nearest few peptidoglycan layers to the membrane surface[19] and so sterically blocks chain extension by transglycosylation through addition of lipid II monomer[6] (Figure 9, panels A and B). This occurs even though there is no direct contact of the tail with lipid II and no well-defined binding site for the headgroup. The disorganization of the bilayer depolarizes the membrane. However, there is no cell lysis induced by plusbacin A_3 and no pore formation (see the Supporting Information).

Membrane depolarization has been reported for telavancin,[20] a vancomycin analogue with a hydrophobic tail much like that of plusbacin A_3. Telavancin inhibits transglycosylation and

forces a disorganization of the membrane leading to depolarization, all without pore formation and cell lysis, although the concentration of drug required is much higher than that for plusbacin A_3.

A general mechanism of membrane depolarization without pore formation is unknown. Perhaps there is a clue in the C{F} REDOR results of Figure 5. The tail-dependent contact of purines with the headgroup of plusbacin A_3 is clear from the REDOR difference spectrum (Figure 5, top left). Purines are presumably in the cytoplasmic ATP, but with plusbacin A_3 in the cell wall, these purines are too distant for effective dipolar contact. However, the dynamics of a thinned and disorganized membrane (Figure 9B) may allow some ATP *entry* into the cell wall (and membrane depolarization) with subsequent binding by plusbacin A_3 headgroups. In addition, purines are brought to the inner membrane surface in ATP-binding cassette (ABC) transporters[21] (Figure 9B). We speculate that drug interaction with a transporter could bring purines within dephasing range of both head and tail (Figure 9C). (In fact, purine C{D} contact with the plusbacin ^{2}H-labeled tail is shown, without comment, in Figure 3 (top right) of ref 4.) A dynamic drug-transporter equilibrium would release ATP to the cell-wall hydrophilic regions where additional drug binding could occur. To account for the observed purine–plusbacin A_3 contact, we therefore propose a dual mode of action: first, inhibition of cell-wall biosynthesis by the well-documented blockage of trans-glycosylation; second, membrane-function disruption by glycan insertion and possible interference with ABC transporters.

Supplementary Material

Refer to Web version on PubMed Central for supplementary material.

Acknowledgments

References

1. Shoji J, Hinoo H, Katayama T, Matsumoto K, Tanimoto T, Hattori T, Higashiyama I, Miwa H, Motokawa K, Yoshida T. Isolation and characterization of new peptide antibiotics, plusbacins A1-A4 and B1-B4. J Antibiot. 1992; 45:817–823. [PubMed: 1500345]

2. Maki H, Miura K, Yamano Y. Katanosin B and plusbacin A(3), inhibitors of peptidoglycan synthesis in methicillin-resistant *Staphylococcus aureus*. Antimicrob Agents Chemother. 2001; 45:1823–1827. [PubMed: 11353632]

3. Wohlrab A, Lamer R, VanNieuwenhze MS. Total Synthesis of Plusbacin A3: A depsipeptide antibiotic active against vancomycin-resistant bacteria. J Am Chem Soc. 2007; 129:4175–4177. [PubMed: 17371023]

4. Kim SJ, Singh M, Wohlrab A, Yu TY, Patti GJ, O'Connor RD, VanNieuwenhze M, Schaefer J. The isotridecanyl side chain of plusbacin-A_3 is essential for the transglycosylase inhibition of peptidoglycan biosynthesis. Biochemistry. 2013; 52:1973–1979. [PubMed: 23421534]

5. Straus SK, Hancock REW. Mode of action of the new antibiotic for Gram-positive pathogens daptomycin: comparison with cationic antimicrobial peptides and lipopeptides. Biochim Biophys Acta Biomembr. 2006; 1758:1215–1223.

6. Cegelski L, Kim SJ, Hing AW, Studelska DR, O'Connor RD, Mehta AK, Schaefer J. Rotational-echo double resonance characterization of the effects of vancomycin on cell wall synthesis in Staphylococcus aureus. Biochemistry. 2002; 41:13053–13058. [PubMed: 12390033]

7. Tong G, Pan Y, Dong H, Pryor R, Wilson GE, Schaefer J. Structure and dynamics of pentaglycyl bridges in the cell walls of Staphylococcus aureus by ^{13}C-^{15}N REDOR NMR. Biochemistry. 1997; 36:9859–9866. [PubMed: 9245418]

8. Gullion T, Schaefer J. Rotational-echo double-resonance NMR. J Magn Reson. 1989; 81:196–200.

9. Bennett AE, Reienstra CM, Auger M, Lakshmi KV, Griffin RG. Heteronuclear decoupling in rotating solids. J Chem Phys. 1995; 103:6951–6958.

10. Stueber D, Mehta AK, Chen Z, Wooley KL, Schaefer J. Local order in polycarbonate glasses by ^{13}C{^{19}F} rotational-echo double-resonance NMR. J Polym Sci Part B: Polym Phys. 2006; 44:2760–2775.

11. Gullion T, Baker DB, Conradi MS. New, compensated Carr-Purcell sequences. J Magn Reson. 1990; 89:479–484.

12. Weldeghiorghis TK, Schaefer J. compensating for pulse imperfections in REDOR. J Magn Reson. 2003; 165:230–236. [PubMed: 14643704]

13. Mueller KT, Jarvie TP, Aurentz DJ, Roberts BW. The REDOR transform: direct calculation of internuclear couplings from dipolar-dephasing NMR data. Chem Phys Lett. 1995; 242:535–542.

14. Seber, GAF., Wild, CJ. Nonlinear Regression. Wiley; New York: 1989.

15. Stueber D, Yu TY, Hess B, Kremer K, O'Connor RD, Schaefer J. Chain packing in polycarbonate glasses. J Chem Phys. 2010; 132:104901-1–104901-9. [PubMed: 20232984]

16. [Date last accessed: Nov 2016] NIST/SEMATECH e-Handbook of Statistical Methods. http://www.itl.nist.gov/div898/handbook/eda/section3/eda3673.htm

17. Kim SJ, Singh M, Preobrazhenskaya M, Schaefer J. Staphylococcus aureus peptidoglycan stem packing by rotational-echo double resonance NMR spectroscopy. Biochemistry. 2013; 52:3651–3659. [PubMed: 23617832]

18. Kim SJ, Cegelski L, Studelska DR, O'Connor RD, Mehta AK, Schaefer J. Rotational-echo double resonance characterization of vancomycin binding sites in Staphylococcus aureus. Biochemistry. 2002; 41:6967–6977. [PubMed: 12033929]

19. Kim SJ, Schaefer J. Hydrophobic side-chain length determines activity and conformational heterogeneity of a vancomycin derivative bound to the cell wall of Staphylococcus aureus. Biochemistry. 2008; 47:10155–10161. [PubMed: 18759499]

20. Lunde CS, Hartouni SR, Janc JW, Mammen M, Humphrey PP, Benton BM. Telavancin disrupts the functional integrity of the bacterial membrane through targeted interaction with the cell wall precursor lipid II. Antimicrob Agents Chemother. 2009; 53:3375–3383. [PubMed: 19470513]

21. Davidson AL, Dassa E, Orelle C, Chen J. Structure, function, and evolution of bacterial ATP-binding cassette systems. Microbiology and Molecular Biology Reviews. 2008; 72:317–364. [PubMed: 18535149]

Abbreviations

C{F}   carbon-channel observation with carbon–fluorine dipolar recoupling

N{F}   nitrogen-channel observation with nitrogen–fluorine dipolar recoupling

N{P}   nitrogen-channel observation with nitrogen–phosphorus dipolar recoupling

REDOR   rotational-echo double resonance
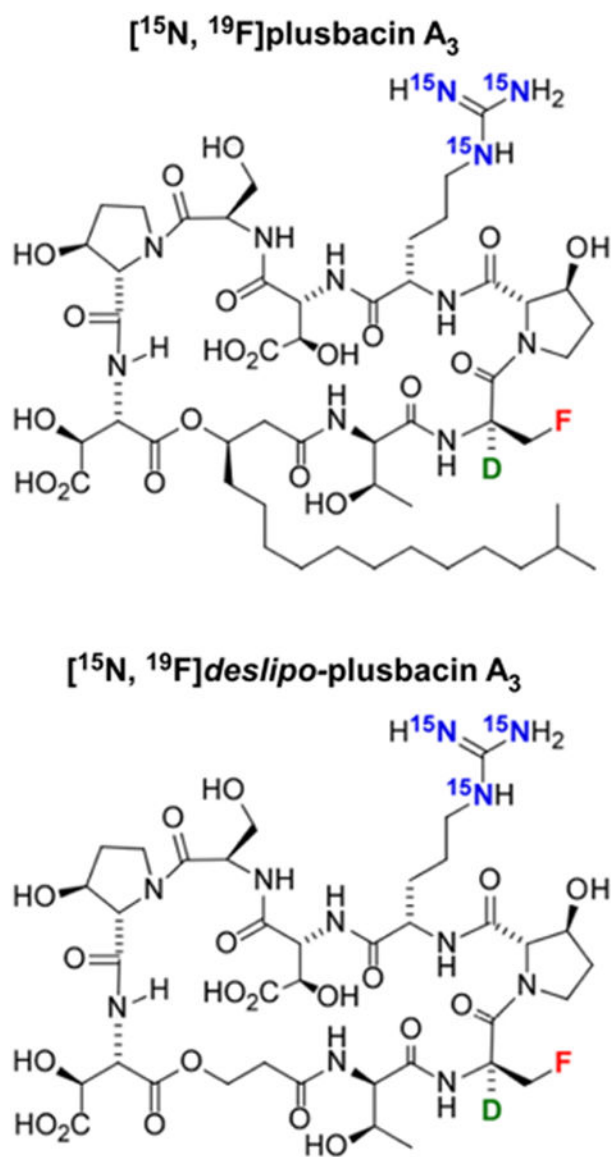
Figure 1.
Chemical structure of double-labeled [^{15}N, ^{19}F]plusbacin A$_3$ and double-labeled [^{15}N, ^{19}F]*deslipo*-plusbacin A$_3$. The deuterium label was not used in this work.
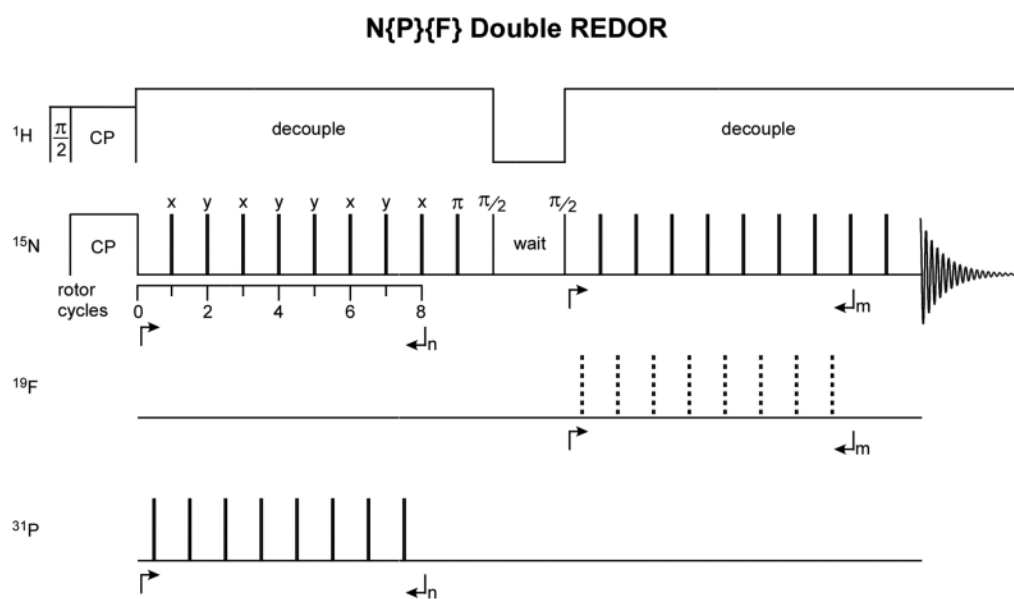
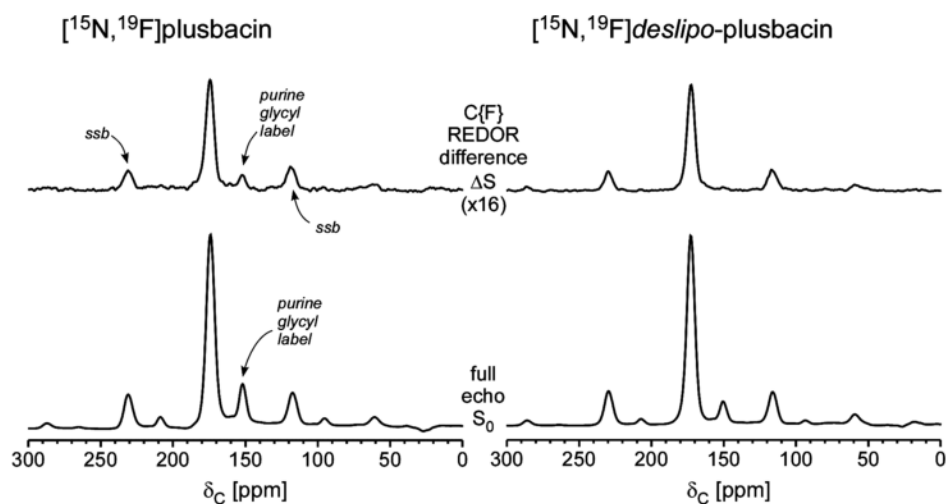**Figure 2.**
Pulse sequence for N{P}{F} double-REDOR NMR. The ^{19}F dephasing pulses (dotted, on for S and off for S_0) follow the ^{31}P dephasing pulses (on for both S and S_0). The wait time can be used as an optional $T_1(N)$ filter. Both refocusing and dephasing pulses follow the xy8 phase alternation scheme.

N{F} REDOR $[^{15}N,^{19}F]$plusbacin A_3
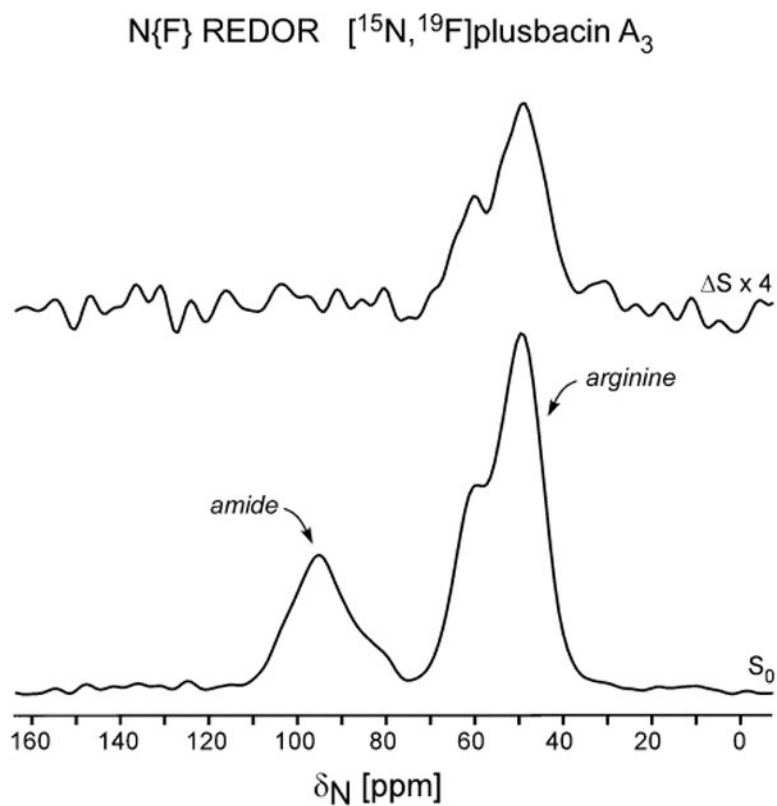
Figure 3.
N{F} REDOR spectra of double-labeled plusbacin A_3 bound to the cell walls of whole cells of *S. aureus* after 8.9 ms of dipolar evolution. The full-echo spectrum is shown at the bottom of the figure and the REDOR difference at the top. The amide-nitrogen peak arises from natural-abundance ^{15}N.
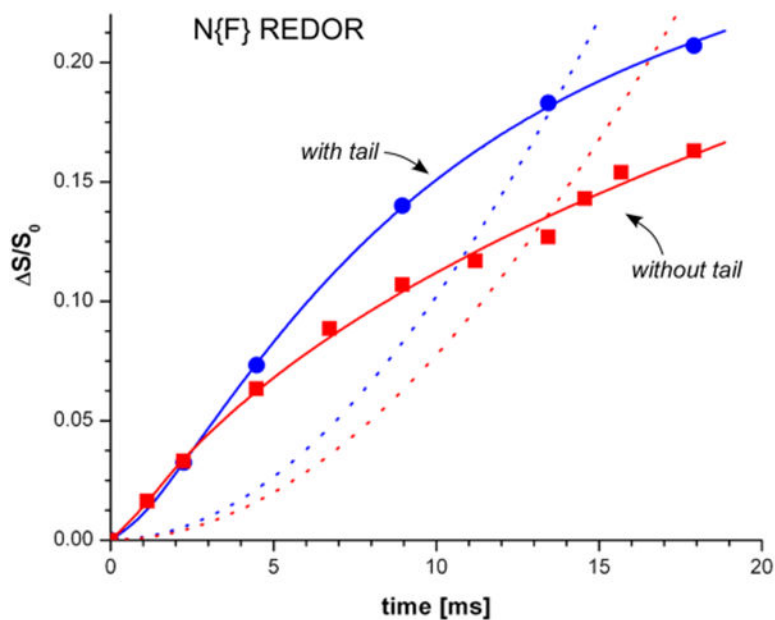
Figure 4.
N{F} REDOR dephasing as a function of dipolar evolution time for double-labeled plusbacin A_3 (five blue symbols) and double-labeled *deslipo*-plusbacin A_3 (10 red symbols) bound to the cell walls of whole cells of *S. aureus* as a function of dipolar evolution time. The solid lines are the dephasings calculated for a bimodal Gaussian distribution of N–F distances, and the dotted lines, for single distances. (See Figure 7 for values of the parameters.) The single-distance calculations can only match a few of the experimental dephasing values.

Figure 5.
C{F} REDOR spectra of double-labeled plusbacin A₃ (left) and of double-labeled *deslipo*-plusbacin (right) each bound to the cell walls of whole cells of *S. aureus* grown in media containing [1-^{13}C]glycine after 8.9 ms of dipolar evolution. The full-echo spectra are shown at the bottom of the figure and the REDOR differences at the top. Most of the ^{13}C label appears in the pentaglycyl bridges of the cell-wall peptidoglycan (172 ppm) and cytoplasmic protein (175 ppm), but some appears in nucleotide purines (153 ppm). Abbreviation: ssb, spinning sideband.
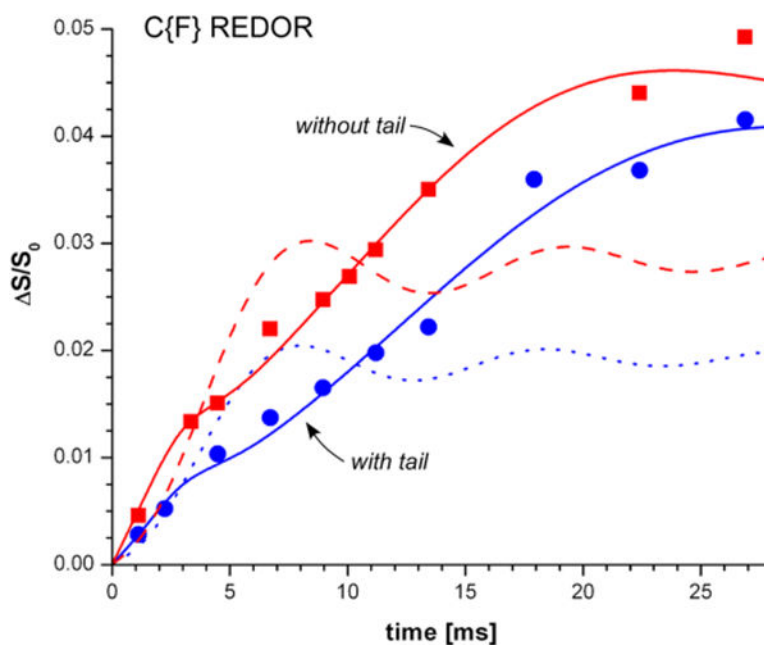
Figure 6.
C{F} REDOR dephasing of the 175 ppm carbonyl-carbon peak as a function of dipolar evolution time for double-labeled plusbacin A_3 (10 blue symbols) and double-labeled *deslipo*-plusbacin A_3 (10 red symbols) bound to the cell walls of whole cells of *S. aureus* grown in media containing $[1-^{13}C]$glycine as a function of dipolar evolution time. The solid lines are the dephasings calculated for a bimodal Gaussian distribution of C–F distances, and the dotted lines, for single distances. (See Figure 7 for values of parameters.) The single-distance calculations can only match a few of the experimental dephasing values.

x{F}[a]	Single distance			Bimodal Gaussian distribution							
	r (Å)	s	χ^2	r_1(Å)	r_2(Å)	σ_1	σ_2	f	s	χ^2	F-test
^{15}N-arg-(with tail)	7	0.95	1.6	12	4.9	0.25	1.8	0.75	0.95	$3 \cdot 10^{-4}$	1937[b]
^{15}N-arg-(without tail)	7.3	0.95	3.0	12	5.7	0.25	4.0	0.72	0.95	0.01	1047[c]
^{13}C-gly-(with tail)	4.9	0.019	1.0	3.8	7.7	0.5	0.5	0.18	0.041	0.10	39[d]
^{13}C-gly-(without tail)	5.1	0.03	1.1	3.7	7.2	0.5	0.5	0.27	0.046	0.03	122[d]

[a]Parameters in gray are fixed, [b]$F_{0.01}(2,2)$=99, [c]$F_{0.01}(2,7)$=9.6, [d]$F_{0.01}(2,6)$=11
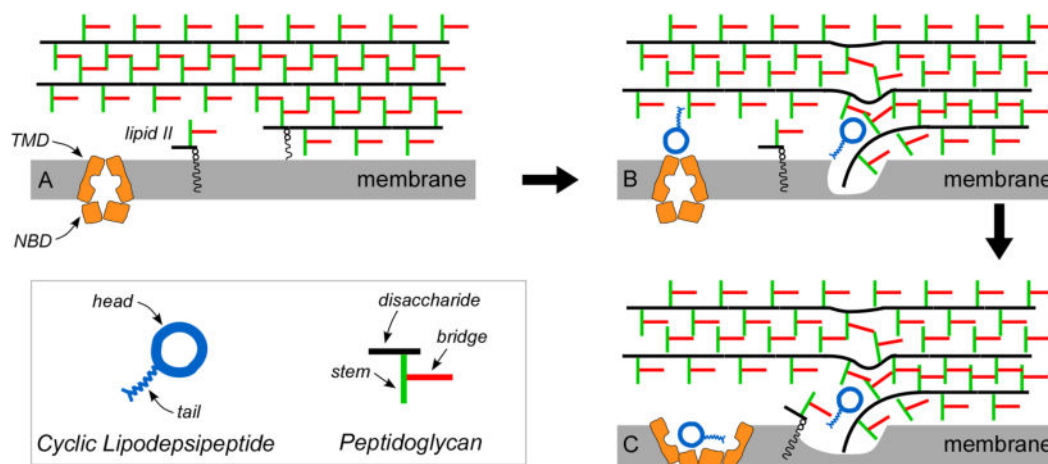
Figure 7.

Parameters for the fit to the REDOR dephasing of Figures 4 (N{F}) and 6 (C{F}) as a function of dipolar evolution time for double-labeled plusbacin A$_3$ (blue numbers from Figures 4 and 6) and double-labeled *deslipo*-plusbacin A$_3$ (red numbers from Figures 4 and 6) bound to the cell walls of whole cells of *S. aureus* grown in media containing [1-^{13}C]glycine, as a function of dipolar evolution time for a single distance (left, white background), and for a bimodal Gaussian distribution of distances (right, shaded background). The parameter s is the asymptotic dephasing limit, χ^2 is a mean-square measure of the deviation of experimental and calculated dephasing, σ is a Gaussian distribution width, and f is the fractional contribution of component 1 (where that of component 2 is $1 - f$). The numbers in gray were fixed. See the text (Materials and Methods) for an explanation of the statistical *F*-test (right-most column) and the critical *F*-distribution numbers given as footnotes to the table.
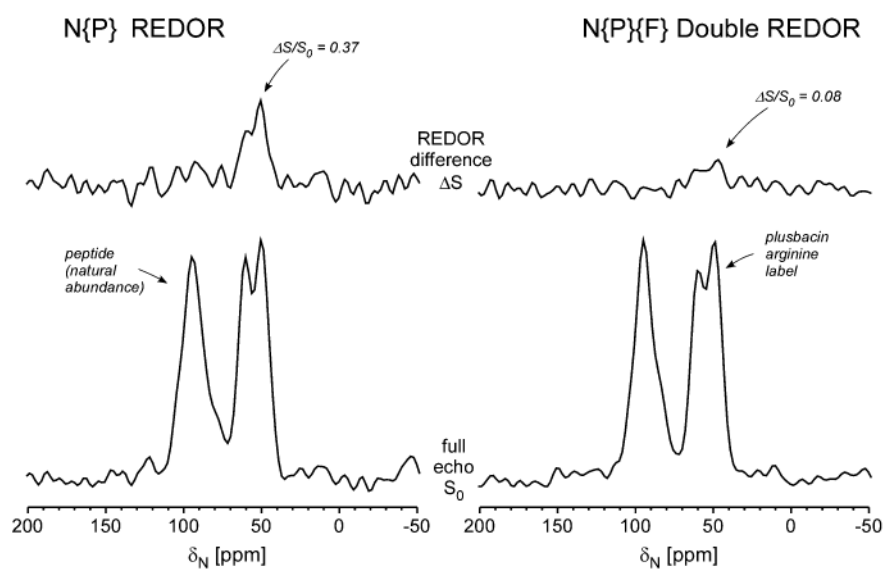
Figure 8.
N{P} REDOR and N{P}{F} double-REDOR spectra of double-labeled plusbacin A_3 bound to the cell walls of whole cells of *S. aureus* after 17.92 ms (left) and 13.44 ms (right) of N–P dipolar evolution using the pulse sequence of Figure 2. The double-REDOR experiment had an additional 4.48 ms of N–F dipolar evolution after a wait of 4 ms. The full-echo spectra are shown at the bottom of the figure and the REDOR differences at the top. The S/S_0 of 8% for the N{P}{F} experiment matches the N{F} value for the same N–F dipolar evolution time of Figure 4 (blue).

Figure 9.
(A) Schematic drawing of the peptidoglycan layers near the bilayer of whole cells of *S. aureus.* (B) The headgroup of plusbascin A_3 inserts near a bridge (red) in the hydrophobic region of the peptidoglycan, and the tail displaces the glycan chain (black) which disorganizes the bilayer. The head-and-tail combination prevents extension of the nascent peptidoglycan by addition of lipid II. (C) A second plusbascin A_3 in the hydrophilic region of the cell wall (see previous panel) is shown blocking the function of an ATP-binding cassette transporter, possibly resulting in proximity of purines in ATP to both plusbacin A_3 head and tail. Abbreviations: TMD, transmembrane domain; NBD, nucleotide-binding domain.